ISSN 0869-2904

EXPERIMENT IN GeoSciences

Mineralogy
Petrology
Geochemistry

Crystallography
Geophysics
Isotopy

2024 Volume **30** Number **1**

INSTITUTE of EXPERIMENTAL MINERALOGY
IEM
RAS
RUSSIAN ACADEMY OF SCIENCES

EXPERIMENT in GeoSciences

Mineralogy
Petrology
Geochemistry

Crystallography
Geophysics
Isotopy

Founded in **1991** by

INSTITUTE of

EXPERIMENTAL

MINERALOGY

Russian Academy of Sciences

EXPERIMENT IN GEOSCIENCES is the only journal in English that gives you the latest, most reliable information on advances in experimental mineralogy, petrology, geochemistry, crystallography and geophysics in Russia. The coverage of the journal includes:

- original research and review articles
- abstracts of scientific papers
- proceedings, abstracts and announcements of national and international conferences, symposia and workshop
- information about the leading experimental centers in Russia
- advertisement of new techniques and equipment

Institute of Experimental Mineralogy

Russian Academy of Sciences
142432 Chernogolovka
Academica Osip'yana str, 4,
Moscow region
Russian Federation

http://www.iem.ac.ru

TRANSLATED into ENGLISH by:
the authors

Ionov A.M. [1], Barkalov O.I. [1], Shulyatev D.A. [2], Gavrilicheva K.A. [1] and Shahlevich O.F. [1] Charoite transformations under thermal treatment

[1]Osipyan Institute of Solid State Physics of the Russian Academy of Sciences, Chernogolovka, Russia (xenia.gavrilicheva@yandex.ru) [2] Materials Modeling and Development Laboratory, NUST MISIS, Leninskiy prospect, 4, 199049 Moscow, Russia

Abstract Structural phase transformations of the charoite mineral induced by thermal treatment at high temperatures were studied by simultaneous monitoring of the thermogravimetry, differential scanning calorimetry, and mass spectrometry curves up and above to its melting temperature range (~ 1300 °C). The chemical composition and phase state of the initial and melted samples were characterized using electron-probe micro-analysis, X-ray powder diffraction, and Raman spectroscopy. It was demonstrated that continuous heating (10 °C/min) up to ~ 600 °C resulting in a mass loss of ~ 5 wt. % was due to crystallization water release and dehydroxylation, while oxygen release and carbonate inclusion decomposition were observed at a higher temperature. The endothermic peak with a heat effect of 82 J/g at 970 ÷ 1050 °C was attributed to the charoite-to-wollastonite transition detected by X-ray powder diffraction in this temperature range. Above 1100 °C, another extended endothermic effect was fixed, which was presumably due to the formation of pseudowollastonite and pre-melting processes. The melting of the charoite sample using the floating zone technique resulted in its transformation to pseudowollastonite and caused a significant color change from lilac to rose pink.

Keywords: *charoite, thermogravimetry, calorimetry, X-ray diffraction, Raman spectroscopy, floating zone melting*

Introduction. Charoite the so-called "lilac miracle of Siberia" is a delightful gemstone (Rogova et al. 2013). This mineral is well-known in the gem market due to its exciting aesthetic properties, such as unique lilac to violet color, structural features, and endemic origin. The main (Russian Federation, Murun massif) deposit "Sirenevyi Kamen" includes both charoite and charoite-containing rocks, with a idealized formula of $(K, Sr, Ba, Mn)_{15–16}(Ca, Na)_{32}[(Si_{70}(O, OH)_{180})](OH, F)_4 \cdot nH_2O$ (Rozhdestvenskaya et al. 2010), and a complex structure of alkaline calcium silicate with tubular Si-O-radicals: $(Ca_{1.57}Na_{0.51}K_{0.93}Ba_{0.07})_{3.11} \cdot Si_4O_{10}(OH_{0.58}F_{0.20})_{0.78} \cdot 0.72H_2O$ (Rogova et al. 2013). The chemical formula of charoite varies among different outcrops, with inclusions of aegirine, tinaksite, microcline, tokkoite and some other minerals of the metasomatic rocks also exhibits a complex association (Reguir 2001). The main charoite element components are K, Na, Ca, Si, and O, F, H_2O, OH, the secondary components are Ba, Sr, and Mn; the presence of traceable amounts of Fe, Mg, Al, Ti, Zr, and Th is discovered in Murun charoite.

To understand the genesis and properties of charoite it is necessary to study the behavior of the mineral upon its heating to high temperatures up to the melting temperature. Moreover, the undoubted interest is to investigate the possibility of charoite crystallization during the melting process. Our study is focused on the high-temperature charoite behavior and the charoite transformation upon melting during crystallization.

Experimental methods and sample characterization. Experiments were conducted using high-quality samples of charoite mineral. To prepare samples for analysis and melting, samples 4x4x40 mm and 4x4x1 mm were cut from a mineral block of high jewelry quality, dark lilac-violet color, without visible white, black and yellow inclusions. The content of elements in charoite was determined at IPTM RAS by inductively coupled plasma atomic emission spectrometry (iCAP-6500, Thermo Scientific, USA) and mass spectral methods of analysis (X Series 2, Thermo Scientific, USA). The elemental composition of the samples was characterized before and after thermal treatment by scanning electron microscopy (SEM, Supra 50 VP with EDX detector, Carl Zeiss).

The Raman spectra were recorded with a Princeton Instruments HRS 500 spectrometer equipped with a liquid nitrogen-cooled charge-coupled device detector. The spectra were monitored with1200 grooves/mm grating. The samples were irradiated at room temperature with a 532-nm KLM-532/SLN-100 DPSS (FTI Optronic, St. Petersburg, Russia) laser with a laser power at the sample of about 5 mW in a back-scattering geometry. A 20x Plan Apo Mitutoyo objective was used to focus the laser beam to a spot of approximately 3 μm in size and collect the scattered light. A razor edge Semrock beam splitter and a Holographic Tydex Notch-6 filter (Tydex, St. Petersburg, Russia) were used for laser line discrimination and acquiring the Raman spectra higher than 200 cm^{-1}. The spectral resolution in the spectral range under study was $\approx 1\ cm^{-1}$. The spectrometer was calibrated using Ne spectral lines with an uncertainty of $\pm 1\ cm^{-1}$.

The X-ray powder diffraction data (XRD) were taken on Rigaku SmartLab SE, Cu-Kα radiation, equipped with 1D D/teX PSD in Bragg-Brentano geometry (Cu-Kα1,2, λ = 1.5418 Å) at room temperature. The data were collected in a 2θ range of 10-90° with a step of 0.01°.

Charoite transformations at high temperatures

were studied experimentally upon heating the samples from room temperature to 1300 °C in the air and argon atmosphere. NETZSCH STA 409 PC/PG was used for simultaneous thermogravimetric and calorimetric analyses from room temperature to a high-temperature of 1300 °C and allowed us to analyze the change in mass, to study the decomposition processes, thermal stability, and behavior during crystallization, and to determine enthalpy transitions, phase transition temperatures. The experiments were performed at a rate of 10.0 °C/min in an alumina crucible in argon.

Charoite rod were remelted by vertical non-crucible floating zone (FZ) melting with optical radiation heating (Balbashov and Egorov 1981).

Results. Charoite composition.. The average chemical composition of the initial charoite sample was SiO_2=52.29%, CaO=31.42%, K_2O=7.60%, Na_2O=4.23%, BaO=2.50% (main components, total 98.04%, Supra 50, EDX detector). Element composition is summarized in Table 1.

Table1. Elemental composition of the charoite samples

	DL (ppm)	Lilac (iCAP-6500)	Lilac (X Series 2)	FZ Melted
Li	0.21	23.1	22.9	19.2
Be	0.21	21.5	16.1	7.18
B	0.79	385	300	<DL
Na	20	---	26000	19236
Mg	2.7	261	226	4.82
Al	200	674	123	21.4
Si	base	320000	309000	278050
K	6	---	48000	69315
Ca	450	190000	155000	158623
Sc	1.1	11.9	12.8	<DL
Ti	23	28.2	21.1	3.03
V	1.6	3.52	31.2	<DL
Cr	0.61	17.9	72.3	<DL
Fe	44	183	186	27.9
Mn	4.2	2709	2540	1904
Ni	0.34	9.51	9.66	0.43
Cu	0.65	69.9	101	7.07
Rb	0.03	330	306	288
Sr	0.06	8200	7660	23281
Y	0.04	100	80.4	71.2
Zr	0.23	46.7	40.7	36
Nb	0.02	4.82	4.05	3.38
Cs	0.02	23.7	18.8	16.9
Ba	0.48	36000	30400	38100
La	0.02	463	357	385
Ce	0.04	928	792	944
Pr	0.01	120	88.4	109
Nd	0.02	470	362	384
Sm	0.01	80.4	63.7	64.6
Eu	0.005	18.2	14.1	15.2
Gd	0.02	49.5	39.6	39.1
Tb	0.01	5.26	4.03	4.05
Dy	0.02	23.9	18.5	19.1
Er	0.01	8.19	6.31	6.66
Yb	0.01	4.75	3.69	3.99
W	0.02	7.72	6.49	0.038
Pb	2.6	64.1	36.5	19.8
U	0.01	18.9	14.1	22

DL – Detection limit

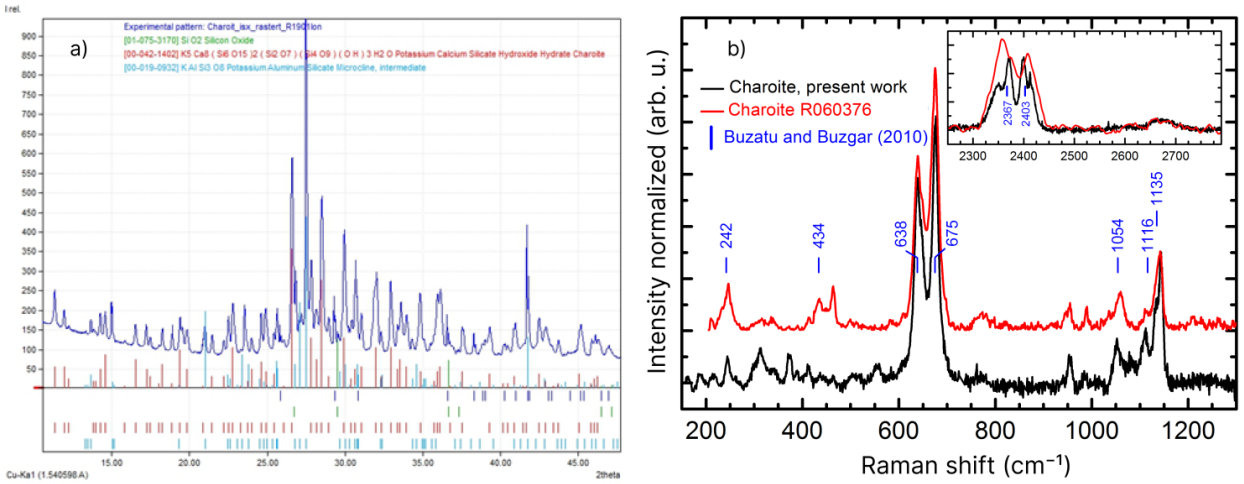

Fig. 1 The initial charoite sample: a) The blue curve is X-ray diffraction pattern ($CuK_{\alpha 1}$ radiation); b) The Raman spectrum of charoite: black - present work, red - RRUFF R060376.

CHAROITE SPECTROSCOPY. The XRD powder pattern and Raman spectrum of the initial charoite sample are presented in Fig. 1 and agree well with the experimental data available in the literature (RRUFF Project database R060376; Buzatu and Buzgar 2010; Rozhdestvenskaya et al. 2010).

Only a few studies were made on charoite (Rogova et al. 1978; Rozhdestvenskaya et al. 2009). The Raman spectra for charoite from the RRUFF (R060376) are similar to the spectrum obtained in the present study. No discussions or detailed vibration mode assignments for this mineral were found in the literature. The Raman spectrum of charoite (Fig. 1, right panel) is characterized by strong fluorescence and background, the peaks are very weak, and only a few of them can be resolved. The peak positions are very close to those reported in (Buzatu and Buzgar 2010). An intensive and broad band around 2400 cm^{-1} is most probably of luminescence origin. It corresponds to the wavelength of ~ 610 nm, i.e., to the red region of the visible light spectrum.

THERMAL TREATMENT. The charoite transformation at high temperatures was studied by heating the samples from RT to 1300 °C in argon and the air. First, a charoite sample placed in the alumina or platinum crucibles was heated in the air in a furnace. After heating above 900 °C in the air, the violet color of charoite began to fade, and the sample melted above 1000 °C. These findings probably indicate that the structural transformations of charoite began above 900 °C and agree with the results of (Nikolskaya et al. 1976), where the charoite sample was discolored completely by annealing under the reducing conditions for three hours at 700 °C.

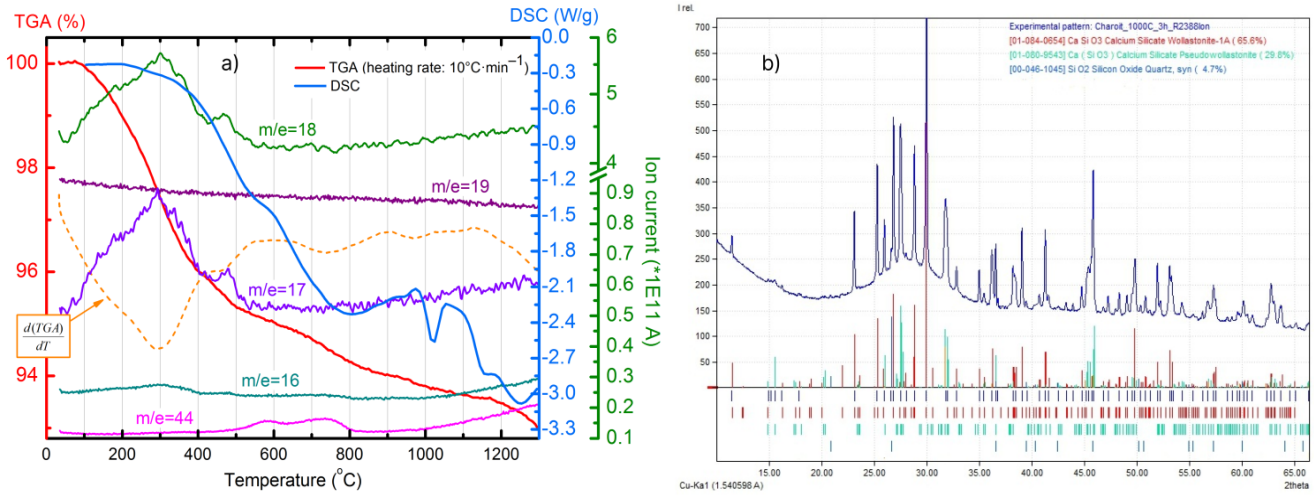

Fig. 2. a) DSC, TGA curves along with the mass spectrometric curves for the initial charoite sample. The dash curve represents the first derivative of the TGA curve; b) XRD pattern of charoite sample annealed at 1000 °C, 3 hours.

As demonstrated by the mass-spectral curves presented in Fig. 2a, upon heating, the water release (m/e = 17, 18) from the charoite sample occurred in a temperature range of ~ 50–600 °C, while there lease of carbon dioxide (m/e = 44) proceeded at 500–800 °C, and that of carbon dioxide and atomic oxygen occurred above ~ 1000 °C.

The thermogravimetric curve measured upon heating charoite shown in Fig. 2a demonstrates singularities at 208, 295, and 460 °C. These values are close to those of our mass spectrometry curves for water (m/e = 18) and hydroxyl group (m/e = 17), as shown in Fig. 2a, and those reported in (Matesanz et al. 2008) for the TGA and DTA dependencies. The DSC curve measured in the present work demonstrates a pronounced endothermic shift right above 200 °C and up to ~ 800 °C. It is featureless in this temperature range probably due to the overlapping of the dehydration, dehydroxylation, and carbonate decomposition processes. A deflection of the first derivative curve of the DSC signal between 500 and 560 °C might point to the peak position of the endothermic processes within this temperature range. The baseline of the DSC signal is more or less leveled above 800°C, and above 900°C two endothermic peaks are observed. The former narrow endothermic peak with the onset at ~ 990 °C and an enthalpy change of 82 J/g should be due to the charoite-to-wollastonite phase transition since the characteristic temperatures determined by the DSC method in the present work coincide with the temperatures obtained by the real-time XRD method and reported in (Janeczek 1991). The mediate sample annealed at 1000 °C for 3 hours is composed of free phases (see Fig. 2b). There are wollastonite (65.6%), pseudowollastonite (29.8%) and a small amount of quartz (~4.7%). We assume that the latter broad heat effect fixed above 1100 °C corresponds to the formation of pseudowollastonite from wollastonite and, probably, its premelting. According to the XRD phase analysis of the charoite samples subjected to isochronic annealing (Marchuk et al. 2016), the first traces of the pseudowollastonite phase appeared at ~ 1050 °C and a single phase state was attained at ~ 1250 °C. On the other hand, the synthetic wollastonite $CaSiO_3$ transforms to pseudowollastonite at 1180°C (Allen et al. 1906). The melting point of the latter phase is 1512 °C (Allen et al. 1906) or 1547 °C (Richet et al. 1998). The endothermic process is obviously not finished at 1300 °C (see Fig. 2); thus, a calorimeter with a higher temperature limit should be used to get a reliable DSC curve.

Hence, our direct mass-spectral and DSC/TGA experimental data confirm the assumptions on the dehydration and dehydroxylation of charoite upon heating. These assumptions were agreed with the results of DSC/TG and IR spectroscopy studies that were reported in (Janeczek 1991; Matesanz et al. 2008; Kaneva et al. 2020).

FLOATING ZONE MELTING. An attempt to grow a bulk polycrystalline sample of charoite is of undoubted interest, allowing for a reliable characterization of its physical properties and studying the high-temperature transformations of this mineral. Assuming that the growth of charoite crystals should apparently be carried out in a hydrothermal environment, in order to study the behavior of charoite under extreme thermal influences, attempts were made to grow a single crystal using non-crucible zone melting in an oxygen atmosphere. Non-crucible floating zone melting (FZM) with radiation heating is a suitable technique for growing high-quality complex oxide single crystals, as demonstrated in (Balbashov and Egorov 1981; Balbashev et al. 1996).

Charoite rod was remelted by vertical non-crucible floating zone (FZ) melting with optical radiation heating. Rods (4x4x40 mm) for FZ melting were prepared by cutting from the deep violet mineral block. The charoite rods were FZ melted in the air, the growth rate was 10–12 mm/h at the beginning, and then 4mm/h. At end of melting 70 mm-long whisker was an easily retracted. As a result, the ingot in the form of cylindrical rods of 35–40 mm in length and 3–4 mm in diameter were obtained. The disk-shaped samples with a thickness of 1 mm and a diameter of 4 mm were prepared by cutting the grown cylindrical rods (see Fig. 3).

The sample color after melting and growth in the air is pale pink-lilac. According to the XRD, there are weak but rather amorphous reflections on the melted part, and the whisker is amorphous. The XRD powder pattern and Raman spectra from central part of ingot of the melted charoite minerals are presented in Fig.4.

The average chemical composition of the melted sample in the middle part (red line area) is SiO_2=62.79%, CaO=24.16%, K_2O=4.28%, Na_2O=8.76% (main components, total 99.99%). Elemental composition is summarized in Table 2.

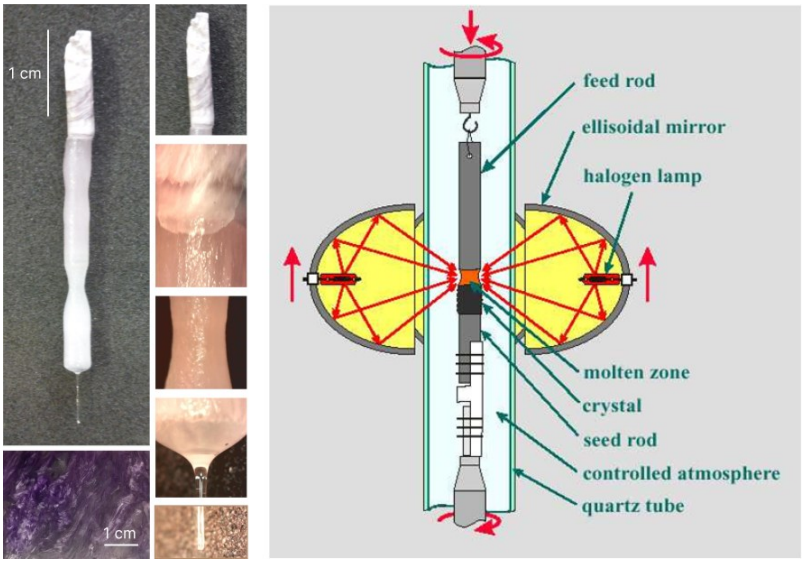

Fig.3 Left: photo of the polished charoite mineral block, the cylinder of charoite (about 40 mm in length and 4 mm in diameter) after melting. Right: non-crucible floating zone scheme.

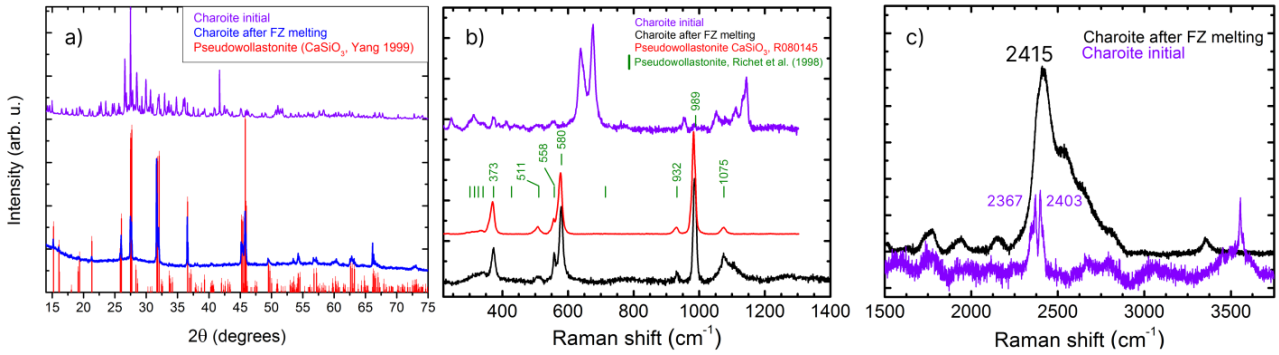

Fig.4. The charoite sample after FZ melting: a) The XRD pattern; b) the Raman spectra; c) the high-frequency part of the Raman spectra.

Table 2. Elemental composition of initial charoite and pseudowollastonite composite ingot melted by FZM

Sample melt	Precursor Charoite violet	Precursor Charoite violet	Thin end melted	Thin end melted	Centre melted	Centre melted	Thick end melted	Thick end melted
Element	Weight%	Atomic%	Weight%	Atomic%	Weight%	Atomic%	Weight%	Atomic%
O K	42.26	61.99	50.70	67.27	46.30	63.88	42.63	60.65
Na K	1.37	1.36	3.78	3.52	2.60	2.49	2.06	2.03
Si K	23.78	19.41	25.84	19.74	28.67	22.85	29.94	24.32
K K	6.45	3.78	7.66	4.32	9.80	5.56	10.22	5.94
Ca K	22.83	13.06	8.40	4.55	8.08	4.48	11.33	6.42
Ba L	2.31	0.39	3.62	0.60	4.55	0.74	3.82	0.64

Standard: O - SiO_2, Na - Albite, Si - SiO_2, K - MAD-10 Feldspar, Ca - Wollastonite, Ba -BaF_2.

Our XRD and Raman data (see Fig. 4) demonstrate the transformation of charoite to high-temperature modification called pseudowollastonite Ca(Na, K, Ba)SiO_3 having a pale pink color upon melting in the air (see also Table 2). An attempt to grow a single crystal of charoite by non-crucible floating zone (FZ) melting in an oxidizing atmosphere was unsuccessful due to the transformation of charoite into pseudowollastonite and its partial amorphization.

By using the tentative mode assignment made for wollastonite by (Buzatu and Buzgar 2010) and for pseudowollastonite by (Richet et al. 1998), the following three frequency ranges might be distinguished in our Raman spectrum of the initial charoite sample and the pseudowollastonite phase (Fig. 4b, c) obtained by the FZ melting procedure. The first one below 500 cm^{-1} corresponds to the metal-oxygen stretching modes, the second one, 500-850 cm^{-1}, refers to the O-Si-O bending and Si-O_{br} stretching vibrations, and the third one, 900-1180 cm^{-1}, corresponds to the SiO_{nbr} stretching vibrations.

However, in the high-frequency region, above 2300 cm^{-1} for charoite and above 1500 cm^{-1} for pseudowollastonite, a series of peaks is observed with a rather intensive broad band in a range of 2500-3000 cm^{-1}. The latter band is not an overtone of the low-frequency modes; thus, we assume it to be due to luminescence with a wavelength of ~ 610 nm, i.e., in the red region of the visible light spectrum.

Conclusions. By measuring simultaneously the weight loss (TGA), heat release (DSC), and mass spectrometry (MS) curves upon heating the charoite sample to 1300 °C, we found that the dehydration and dehydroxylation processes (water and hydroxyl group release, m/e = 17, 18) occurred at 50 – 460 °C. It should be noted that after dehydration and dehydroxylation (loss of 5 %) at 50 – 500 °C charoite structure still exist according XRD and Raman data. Carbon dioxide release (m/e = 44) observed in a temperature range of 500–800 °C was probably due to decomposition of the carbonate inclusion in the mineral, and the heated sample lost oxygen (m/e = 16) above 1000 °C. The endothermic peak monitored at 970 – 1055 °C with an integral enthalpy change of 82 J/g was due to the formation of wollastonite from charoite. The melting of charoite by the floating zone procedure resulted in its transition to a pseudowollastonite-like phase.

Acknowledgments

The authors would like to thank the Shared Facilities Center at the Osipyan Institute of Solid State Physics RAS (Chernogolovka) for the use of the micro-Raman optical system and Rigaku SmartLab SE diffractometer. This work was carried out within the framework of the Governmental Program of Osipyan Institute of Solid State Physics RAS.

References

Allen ET, White WR, Wright FE (1906) On wollastonite and pseudo-wollastonite, polymorphic forms of calcium metasilicate, with optical study by F. E. Wright. American Journal of Science s4-21:89–108. https://doi.org/10.2475/ajs.s4-21.122.89

Balbashev AM, Shulyatev DA, Panova GKh, et al (1996) The floating zone growth and superconductive properties of $La_{1.85}Sr_{0.15}CuO_4$ and $Nd_{1.85}Ce_{0.15}CuO_4$ single crystals. Physica C: Superconductivity 256:371–377. https://doi.org/10.1016/0921-4534(95)00647-8

Balbashov AM, Egorov SK (1981) Apparatus for growth of single crystals of oxide compounds by floating zone melting with radiation heating. Journal of Crystal Growth 52:498–504. https://doi.org/10.1016/0022-0248(81)90328-6

Buzatu A, Buzgar N (2010) THE RAMAN STUDY OF SINGLE-CHAIN SILICATES. Analele Stiintifice ale Universitatii "Al I Cuza" din Iasi Seria Geologie LVI:107–125

Janeczek J (1991) Thermal decomposition of charoite. Mineralogia Polonica 22:21–27

Kaneva EV, Radomskaya TA, Shendrik RYu, et al (2020) FTIR, XRF and Powder XRD Experimental Study of Charoite: Crystal Chemical Features of Two Associated Generations. In: Votyakov S, Kiseleva D, Grokhovsky V, Shchapova Y (eds) Minerals: Structure, Properties, Methods of Investigation. Springer International Publishing, Cham, pp 97–104

Marchuk MV, Medvedev VYa, Ivanova LA, et al (2016) CHAROITE. EXPERIMENTAL STUDIES. Geodin tektonofiz 7:105–118. https://doi.org/10.5800/GT-2016-7-1-0199

Matesanz E, Garcia-Guinea J, Crespo-Feo E, et al (2008) THE HIGH-TEMPERATURE BEHAVIOR OF CHAROITE. The Canadian Mineralogist 46:1207–1213. https://doi.org/10.3749/canmin.46.5.1207

Nikolskaya L, Novozhilov A, Samoilovich M (1976) On the nature of colours of the new alkaline calcium silicate from the Eastern Transbaikalia. Izv AN SSSR 116–120

Richet P, Mysen BO, Ingrin J (1998) High-temperature X-ray diffraction and Raman spectroscopy of diopside and pseudowollastonite. Physics and Chemistry of Minerals 25:401–414. https://doi.org/10.1007/s002690050130

Rogova V, Rogov Y, Drits V, Kuznetsova N (1978) Charoite — a new mineral, and a new jewelery stone. Zapiski Vsesoyuznogo Mineralogicheskogo Obshchestva 107:94–100.

Rogova V, Rozhdestvenskaya I, Vorobjov E, et al (2013) Charoite. The Lilac Miracle of Siberia. Illustrated popular science book, 2nd edn. Petrografika, Irkutsk

Rozhdestvenskaya I, Mugnaioli E, Czank M, et al (2010) The structure of charoite, $(K,Sr,Ba,Mn)_{15-16}(Ca,Na)_{32}[(Si_{70}(O,OH)_{180})]$ $(OH,F)_{4.0}.nH_2O$, solved by conventional and automated electron diffraction. Mineral mag 74:159–177. https://doi.org/10.1180/minmag.2010.074.1.159

Rozhdestvenskaya IV, Kogure T, Abe E, Drits VA (2009) A structural model for charoite. Mineral mag 73:883–890. https://doi.org/10.1180/minmag.2009.073.2.883

Rodkin M.V.[1], Punanova S.A.[1], Martynova G.S.[2] Trace element composition of natural objects. *UDC 5*50.4.41

[1]Oil and Gas Research Institute Russian Academy of Sciences, Moscow (rodkin@mitp.ru); [2] Institute of Geology and Geophysics, Ministry of Science and Education of Azerbaijan

Abstract The paper presents the results of geochemical studies of the products of activity of mud volcanoes and of oil deposits on the western side of the South Caspian depression. The trace elements (TE), hydrocarbon and component compositions of naphthides from the Absheron, Shamakhi-Gobustan and Nizhnekura regions of Azerbaijan have been examined. Comparison of the TE contents in oils and in oil mud volcanic fluids, as well as isotopic characteristics and biomarkers indicates a common genesis